Chinese Physics B

PAPER

Degenerate antiferromagnetic states in spinel oxide LiV_2O_4*

To cite this article: Ben-Chao Gong *et al* 2020 *Chinese Phys. B* **29** 077508

Degenerate antiferromagnetic states in spinel oxide LiV_2O_4*

Ben-Chao Gong(龚本超)[1], Huan-Cheng Yang(杨焕成)[2,1], Kui Jin(金魁)[3,4], Kai Liu(刘凯)[1,†], and Zhong-Yi Lu(卢仲毅)[1,‡]

[1] *Department of Physics and Beijing Key Laboratory of Opto-electronic Functional Materials & Micro-nano Devices, Renmin University of China, Beijing* 100872, *China*

[2] *Beijing Computational Science Research Center, Beijing* 100193, *China*

[3] *Beijing National Laboratory for Condensed Matter Physics, Institute of Physics, Chinese Academy of Sciences, Beijing* 100190, *China*

[4] *Collaborative Innovation Center of Quantum Matter, Beijing* 100190, *China*

(Received 5 March 2020; revised manuscript received 18 May 2020; accepted manuscript online 25 May 2020)

The magnetic and electronic properties of spinel oxide LiV_2O_4 have been systematically studied by using the spin-polarized first-principles electronic structure calculations. We find that a series of magnetic states, in which the ferromagnetic (FM) V_4 tetrahedra are linked together through the corner-sharing antiferromagnetic (AFM) V_4 tetrahedra, possess degenerate energies lower than those of other spin configurations. The large number of these energetically degenerated states being the magnetic ground state give rise to strong magnetic frustration as well as large magnetic entropy in LiV_2O_4. The corresponding band structure and density of states of such a typical magnetic state in this series, i.e., the ditetrahedron (DT) AFM state, demonstrate that LiV_2O_4 is in the vicinity of a metal–insulator transition. Further analysis suggests that the t_{2g} and e_g orbitals of the V atoms play different roles in the magnetic exchange interactions. Our calculations are consistent with previous experimental measurements and shed light on understanding the exotic magnetism and the heavy-fermion behavior of LiV_2O_4.

Keywords: spinel oxide, magnetic properties, heavy fermion, first-principles calculations

PACS: 75.47.Lx, 75.30.Mb, 71.20.−b **DOI:** 10.1088/1674-1056/ab9617

1. Introduction

The transition metal spinel compounds AB_2C_4 have attracted broad interest due to their versatile physical properties that originate from the intimate interplay of the charge, spin, orbital, and lattice degrees of freedom. There exist different forms of spinels.[1] In the normal spinels, the *A* cations occupy the tetrahedral sites and the *B* cations occupy the octahedral sites. In the inverse spinels, the tetrahedral site is occupied by *B* cations, while the octahedral site is shared between *A* and *B* cations. Among the normal spinels, there are superconducting $LiTi_2O_4$,[2–5] charge-ordering $LiMn_2O_4$,[6,7] antiferromagnetic ZnV_2O_4,[8] spin-orbital-liquid $FeSc_2S_4$,[9] ferroelectric $Fe_{1-x}Mn_xV_2O_4$,[10] etc. One typical normal spinel oxide LiV_2O_4 is known as the first d-electron heavy fermion (HF) compound, which shows a large electronic specific-heat coefficient of 420 mJ/(K^2·mol) and an enhanced quasi-particle mass compared with conventional metals.[11] While in general the HF behavior is observed in the compounds containing rare earth elements with highly localized f electrons, the unexpected discovery of HF behavior in LiV_2O_4 with only d electrons has inspired numerous experimental and theoretical studies in the past two decades.[11–47] Nevertheless, the underlying mechanism of the HF behavior in LiV_2O_4 has not reached a consensus.

One scenario concerns about the Kondo effect as the one in a typical HF compound.[12] In LiV_2O_4, the crystal field effect splits the V 3d orbitals into the threefold t_{2g} and the twofold e_{2g} orbitals, and then the trigonal point-group symmetry on the V atom further splits the t_{2g} orbitals into the one-fold a_{1g} and the twofold $\acute{e}_g$ parts.[13–15] Since there are one and a half 3d electrons on each $V^{3.5+}$ ion, one d electron occupies the lower-energy a_{1g} orbital while the remaining d electron resides on the $\acute{e}_g$ orbital.[14] The Kondo coupling between the local a_{1g} electrons and the itinerant $\acute{e}_g$ electrons, which mimics the coupling between localized f electrons and itinerant conduction electrons in a conventional HF compound, was proposed to be responsible for the HF behavior observed in LiV_2O_4.[14] However, it should be noted that by using the local density approximation plus dynamical mean field theory (LDA + DMFT) calculations, Arita and coworkers suggested that the HF behavior in LiV_2O_4 is only related to the relatively local a_{1g} orbitals rather than the hybridization between the a_{1g} and $\acute{e}_g$ orbitals.[16]

Another standpoint focuses on the spin and/or orbital fluctuations in consideration of the geometrical frustration in LiV_2O_4.[17–19] Although there is neither long-range magnetic order nor structural phase transition under all measuring

*Project supported by the National Key R&D Program of China (Grant Nos. 2017YFA0302903 and 2019YFA0308603), the National Natural Science Foundation of China (Grant Nos. 11774422, 11774424, and 11674374), the CAS Interdisciplinary Innovation Team, the Fundamental Research Funds for the Central Universities, China, and the Research Funds of Renmin University of China (Grant No. 19XNLG13).

†Corresponding author. E-mail: kliu@ruc.edu.cn

‡Corresponding author. E-mail: zlu@ruc.edu.cn

temperatures,[11,20,21] the negative Curie–Weiss temperature derived from the magnetic susceptibility experiment[11,22] indicates the existence of antiferromagnetic (AFM) spin interactions in LiV_2O_4. This is also consistent with the measurements of neutron scattering, nuclear magnetic resonance (NMR), and muon spin rotation/relaxation/resonance (μSR).[23,24] Recently, an orbital-selective NMR study suggested that a frustrated spin liquid, which is formed by the orbital-dependent local moments coupling with the itinerant electrons via the Hund's effect, is relevant to the HF behavior.[24] In addition, a time-of-flight inelastic neutron scattering experiment revealed two peaks of the scattering intensity in the moment–energy space and proposed that the spin–orbit fluctuations are highly possible based on the V ditetraheron.[17] Nevertheless, there is no density functional theory (DFT) study about the ditetrahedron magnetic configuration in LiV_2O_4. Is it the spin pattern that causes the exotic properties of LiV_2O_4, or even is the driving mechanism of its HF behavior?

In this work, we have performed first-principles studies on the magnetic and electronic properties of the spinel oxide LiV_2O_4. We find a series of ditetrahedron antiferromagnetic states with the degenerate energies lower than those of other magnetic states. The magnetic mechanism is analyzed based on the density of states and the charge densities. The enlightment of our calculations on the exotic properties of LiV_2O_4 is further discussed.

2. Computational details

The spin-polarized first-principles electronic structure calculations were performed by using the projector augmented wave (PAW) method[48,49] as implemented in the VASP package.[50–53] For the exchange–correlation functional, the generalized gradient approximation (GGA) of Perdew–Burke–Ernzerhof (PBE) type[54] was employed. The kinetic energy cutoff of the plane-wave basis was set to 520 eV. A fully variable-cell relaxation for the cubic cell of LiV_2O_4 was first carried out to obtain the equilibrium lattice parameters. The internal atomic positions were relaxed with the quasi-Newton algorithm and the PBE functional until the forces on all atoms were smaller than 0.01 eV/Å. Different supercells were used to study various spin configurations. For the Brillouin zone (BZ) sampling of the $1\times1\times1$ and $2\times1\times1$ supercells, the $8\times8\times8$ and $4\times8\times8$ k-point meshes were adopted, respectively. The Gaussian smearing method with a width of 0.05 eV was utilized for the Fermi surface broadening. The density of states (DOS) and total energies were also checked by using the tetrahedron method with Blöchl corrections,[55] which does not change our conclusions. At the equilibrium structure of LiV_2O_4, due to the well-known underestimation of band gaps by using the GGA functional, the electronic structures were examined with the modified Becke–Johnson (MBJ) exchange potential[56,57] in combination with the GGA correlation at the meta-GGA level of Jacob's ladder for density functional approximation.[58]

3. Results and analysis

Spinel oxide LiV_2O_4 has a face-centered cubic (FCC) structure with the $Fd\bar{3}m$ space group symmetry (Fig. 1). Each V atom is coordinated by six O atoms, forming a VO_6 octahedron. The 3d orbitals of each V atom in LiV_2O_4 own 1.5 electrons according to the valence counting, which indicates that there may exist local magnetic moment on the V atom. As references, the nonmagnetic (NM) and ferromagnetic (FM) states were first studied. Considering that V atoms form a geometrically frustrated pyrochlore lattice and four nearest-neighboring V atoms constitute a V_4 tetrahedron in LiV_2O_4, three typical AFM spin configurations denoted respectively as the AFM1, AFM2, and AFM3 states in Figs. 1(b)–1(d) were further investigated. The common feature among these AFM states is that there are two spin-up and two spin-down V atoms in each V_4 tetrahedron, while the difference among them is that there exist different numbers of spin-up and spin-down V atoms in a V_4 chain along the $[0\,1\,1]$ direction. In addition to the AFM V_4 tetrahedrons in Figs. 1(b)–1(d), the V atoms may also couple ferromagnetically in a V_4 tetrahedron,[17] which gives rise to a ditetrahedron (DT) AFM state as shown in Fig. 1(a).

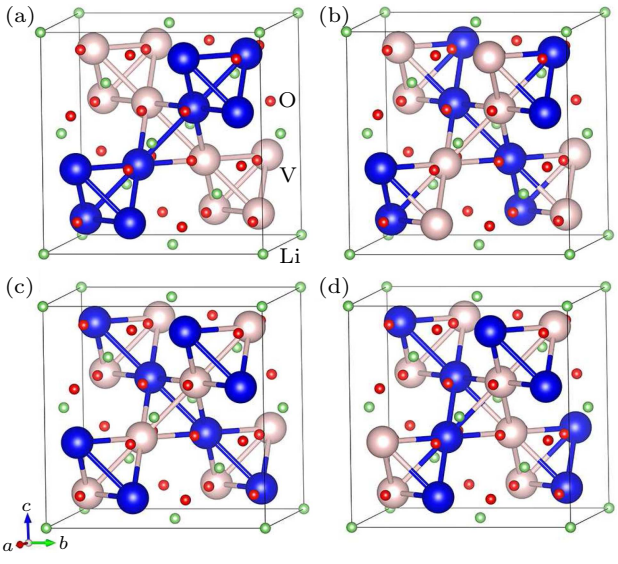

Fig. 1. Four different spin configurations of LiV_2O_4 in a $1\times1\times1$ cubic cell: (a) DT AFM state, namely, the ferromagnetic V_4 tetrahedral clusters connecting each other with the corner-sharing AFM V_4 tetrahedra, (b) AFM1, (c) AFM2, and (d) AFM3 states. Here, the green, red, pink, and blue balls denote the Li, O, spin-up V, and spin-down V atoms, respectively.

The calculated energies of these magnetic states with respect to that of the nonmagnetic state are listed in Table 1. As is seen, all magnetic states are energetically more stable

than the nonmagnetic state. Among them, the DT AFM state owns the lowest energy, which is about 24 meV/V lower than that of the AFM1 state. Moreover, the AFM1 state is at least 13 meV/V lower than the AFM2, AFM3, and FM states. The energy sequence of the AFM1, FM, and NM states from our calculations is in accord with the previous result.[30] Nevertheless, the DT AFM state with the lowest-energy has not been studied in preceding DFT calculations.[13–16,29–31]

Table 1. Relative energies E_{total} (in units of meV per V atom) of the AFM1, AFM2, AFM3, FM, and a series of DT AFM states with respect to the nonmagnetic state for LiV_2O_4 calculated with the PBE functional at the GGA level. One case is with fully relaxed lattice parameters and internal atomic positions, the other is in perfect cell with experimental lattice constants ($a = b = c = 8.255$ Å[43] and high-symmetry atomic positions. The corresponding average local moments M (in units of μ_B) on V atoms are also listed.

Spin configurations	Fully relaxed		Perfect cell	
	E_{total}	M	E_{total}	M
AFM1	−154.9	1.25	−104.1	1.13
AFM2	−142.6	1.21	−79.6	1.10
AFM3	−137.0	1.20	−83.5	1.08
FM	−150.7	1.36	−130.0	1.41
DT (DT1)	−179.4	1.32	−138.1	1.29
DT2	−179.6	1.32	−138.0	1.29
DT3	−179.6	1.32	−138.2	1.29
DT4 (supercell)	−179.4	1.33		

Since there is no long-range magnetic order observed in LiV_2O_4 even down to 0.02 K,[11] we would like to know whether or not there are low-lying magnetic states competing with the DT AFM state [Fig. 1(a)]. We studied three representative spin configurations that all possess the corner-sharing ferromagnetic V_4 tetrahedra, i.e., the DT1, DT2, and DT3 AFM states shown in Fig. 2. Actually, the DT1 AFM state is generated by doubling the cubic cell of the DT AFM state [Fig. 1(a)] along a direction. From the total energies of these states (Table 1), it can be concluded that these DT series of AFM states have almost degenerate energies. On the other hand, previous experiment showed that LiV_2O_4 has small structural distortions in the VO_6 octahedron.[24] We have thus investigated the influence of minor lattice distortions on the DT series of states. In comparison with the above results calculated with the relaxed internal atomic positions (Table 1), the relative energies of different magnetic states for perfect LiV_2O_4 with high-symmetry atomic positions demonstrate that the DT series of states still hold the lowest degenerate energies (Table 1). This suggests that the robust magnetically disordered state is irrelevant to the Jahn–Teller effect of lattice structure. Evidently, if the supercell is further expanded, more energetically degenerated DT-like AFM states would be found, as verified by our calculations in a $2 \times 2 \times 1$ supercell (Table 1). In other words, the DT series of AFM states, in which FM V_4 tetrahedra are linked together through the corner-sharing AFM V_4 tetrahedra, have degenerate energies lower than those of other spin configurations and thus constitute the magnetic ground state of LiV_2O_4. This leads to strong magnetic frustration in LiV_2O_4 and results in the absence of long-range magnetic order.[11,20]

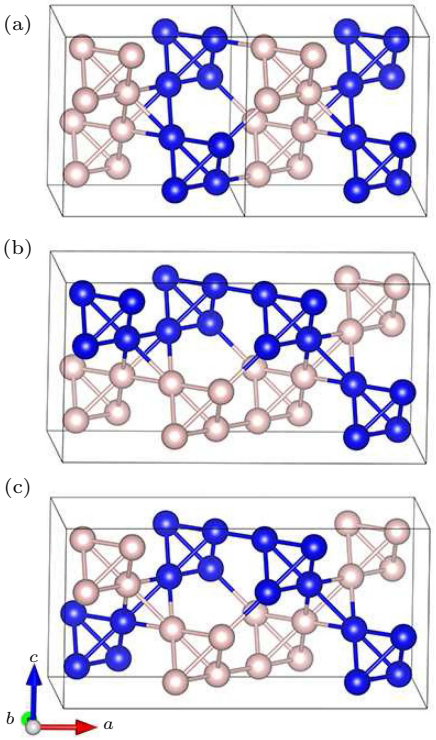

Fig. 2. Three representative spin configurations of LiV_2O_4 in a $2 \times 1 \times 1$ supercell with the corner-sharing ferromagnetic V_4 tetrahedra: (a) DT1 (DT) state, (b) DT2 state, and (c) DT3 state. The pink and blue balls denote the spin-up and spin-down V atoms, respectively. The Li and O atoms have been omitted for clarity.

Among the DT series of magnetic states, we take the DT AFM state [Fig. 1(a)] as a representative case to study the electronic structure of the ground state. Figure 3 shows the primitive cell and corresponding BZ for the DT AFM state of LiV_2O_4. Note that the magnetic cell is the same as the primitive cell. The band structure along the high-symmetry paths of BZ calculated with the PBE functional is demonstrated in Fig. 4(a). Distinct from previous non-spin-polarized calculations,[13–16,29,30] we find that for the DT AFM state only one band slightly crosses the Fermi level. The small density of states (DOS) around the Fermi level suggests that LiV_2O_4 is in the vicinity of a metal–insulator transition. In addition to the PBE calculations at the GGA level, we also examined the electronic structure with the MBJ potential at the meta-GGA level [Fig. 4(b)] as well as the GGA+U method (not shown). The MBJ potential and the GGA+U method yield the band gaps of ~ 0.25 eV and ~ 0.12 eV, respectively, both of which overestimate the band gap compared with the experiments.[32,33,39] Our calculations show that LiV_2O_4 is close to a magnetic insulator, which explains its bad-metal behavior found in experiments.[39,40]

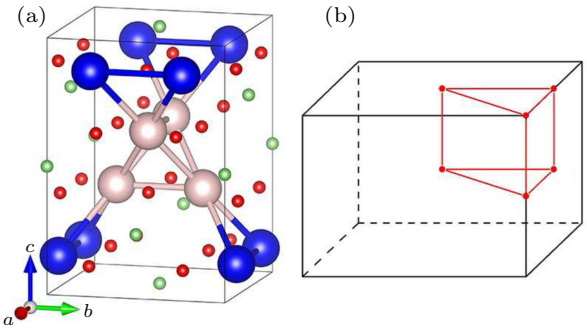

Fig. 3. (a) Primitive cell and (b) Brillouin zone for the DT AFM state of LiV_2O_4. The green, red, pink, and blue balls denote the Li, O, spin-up V, and spin-down V atoms, respectively. The high-symmetry points in Brillouin zone are indicated by red dots.

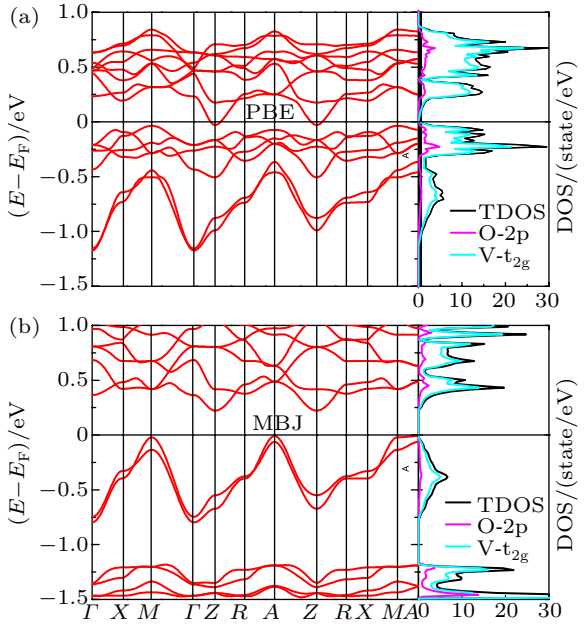

Fig. 4. Band structure along high-symmetry paths of Brillouin zone and total density of states (DOS) for the DT AFM state of LiV_2O_4 calculated with (a) the PBE functional at the GGA level and (b) the MBJ potential at the meta-GGA level.

In order to study the magnetic interactions in the DT AFM state of LiV_2O_4, we calculated the partial density of states (PDOS) for the Li, V, O-12, and O-22 atoms (Fig. 5). Due to the crystal field effect, the V 3d orbitals split into the higher-energy twofold e_g orbitals and the lower-energy threefold t_{2g} orbitals with a 1.2 eV energy interval. Moreover, the partially occupied V e_g orbitals in the energy range from -8 eV to -2 eV hybridize with the O 2p orbitals. This p–d hybridization can be seen more clearly from the band-decomposed charge densities in the same energy range [Fig. 6(a)], for which the charge densities of the V e_g orbitals connect with those of adjacent O 2p orbitals. The superexchange via the bridging O atom, which stems from the p–d hybridization in the energy range from -8 eV to -2 eV, can induce the AFM interactions between the V spins.

On the other hand, the PDOS in the energy range from -1.5 eV to 0 eV mainly consists of V t_{2g} orbitals [Fig. 5(b)]. From the corresponding band-decomposed charge densities in Fig. 6(b), we can see that the charge densities of the V atoms point towards the center of the V_4 tetrahedron and tend to overlap with each other. Meanwhile, there are two kinds of O atoms: one is on top of the ferromagnetic V triangles, such as O-12, whose major charge densities point towards Li-1 atom; the other is on top of the antiferromagnetic V triangles, such as O-22, whose charge densities point towards Li-18 atom. The bonding between the Li and O atoms is also evidenced by the PDOS shown in Fig. 5(a), in which small peaks of Li just below the Fermi level overlap with the O states. These results indicate that the hybridization between V t_{2g} orbitals and O 2p orbitals in the energy range from -1.5 eV to 0 eV is very weak. Instead, the direct overlap of V t_{2g} orbitals can contribute to the FM interactions between the V spins.

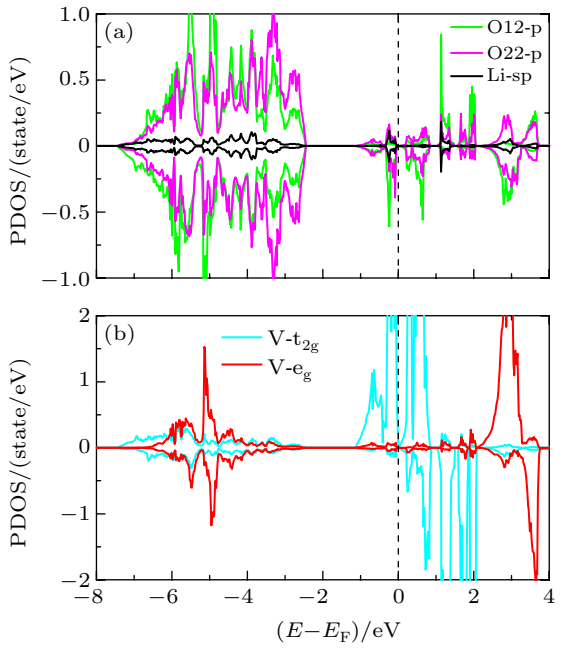

Fig. 5. Partial density of states for the V, Li, O-12, and O-22 atoms [labeled in Fig. 6(b)] in the DT AFM state of LiV_2O_4 calculated with the PBE functional at the GGA level. The Fermi level sets to zero.

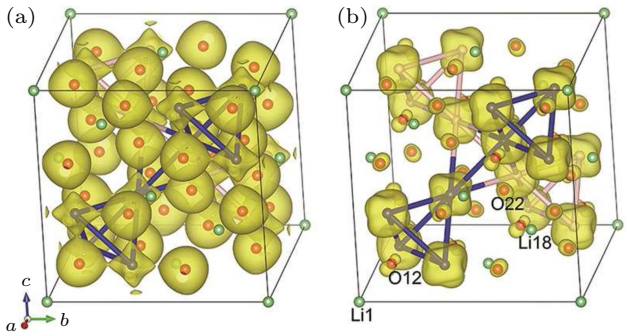

Fig. 6. Band-decomposed charge densities in the energy range from (a) -8 eV to -2 eV and (b) -1.5 eV to 0 eV for the DT AFM state of LiV_2O_4 calculated with the PBE functional at the GGA level. The green, red, pink, and blue spheres denote the Li, O, spin-up V, and spin-down V atoms, respectively.

4. Discussion

Our calculations demonstrate that in spinel oxide LiV_2O_4 there are a series of DT AFM states with the degenerate lowest energies (Table 1), in which the ferromagnetic V_4 tetrahedra formed by four nearest-neighboring V atoms are linked together by the corner-sharing antiferromagnetic V_4 tetrahedra [Figs. 1(a) and 2]. In real LiV_2O_4 material, it can be inferred that the degeneracy of the DT-like magnetic states would increase enormously. The large number of energetically degenerated magnetic states result in strong spin fluctuations and isotropic interactions. This explains the experimental findings that neither static magnetic order nor structural phase transition is observed in LiV_2O_4 down to very low temperature,[11,34] and also coincides with the proposal of spin-liquid behavior in LiV_2O_4.[24] Similar energy degeneracies of the low-lying magnetic states have been found in our previous studies on β-FeSe[59] and α-$RuCl_3$,[60] while the former has no long-range magnetic order and the latter is close to the magnetic disordered state. It is also worth noting that our finding about the magnetic ground state of LiV_2O_4, which consists of the DT series of AFM states, agrees well with the ditetrahedron-based AFM fluctuations as suggested by recent time-of-flight inelastic neutron scattering experiment.[17]

From the electronic structure of the magnetic ground state of LiV_2O_4 (Figs. 4 and 5), we can see that LiV_2O_4 is in the vicinity of a metal–insulator transition. The small density of states at the Fermi level is in line with the experimental observations that LiV_2O_4 is a bad metal[32,33] and has relatively higher resistivity (a few mΩ·cm) than ordinary metals.[39] In addition, there is a sharp peak in the PDOS of V atom right below the Fermi level [Fig. 5(b)], indicating the strong localization of V 3d orbitals. Both the orbital localization and the influence of aforementioned AFM spin fluctuations on itinerant carriers may be relevant to the mass enhancement of quasiparticles and the heavy-fermion behavior in LiV_2O_4.[24,36]

As to the magnetic mechanism in LiV_2O_4, the 3d orbitals on each V atom in the VO_6 octahedron have been splitted to the e_g and t_{2g} components due to the crystal field effect [Fig. 5(b)]. The partially occupied V e_g orbitals in the energy range from -8 eV to -2 eV hybridize with the O 2p orbitals [Fig. 6(a)], which results in the AFM superexchange between the V spins via the bridging O atoms.[30] On the other hand, the t_{2g} orbitals on neighboring V atoms of the V_4 tetrahedron in the energy range of -1.5 eV to 0 eV all point to the center of the tetrahedron and tend to directly overlap with each other[30] [Fig. 6(b)], which is favorable for the FM coupling. So the e_g and t_{2g} orbitals of the V atoms play different roles in the magnetic interactions. The competition between these magnetic interactions as well as the geometric frustration in LiV_2O_4 leads to strong spin fluctuations. In fact, both FM and AFM spin fluctuations in LiV_2O_4 have been observed by previous experiments.[17,23,24,35–38]

5. Conclusions

In summary, based on spin-polarized first-principles calculations, we have found that in the spinel oxide LiV_2O_4 there are a series of ditetrahedron magnetic states with corner-sharing FM and AFM V_4 tetrahedra that have the degenerate lowest energies. The random combinations of these states constitute the magnetic ground state of LiV_2O_4, which does not develop any static magnetic order. The magnetic and geometric frustrations in LiV_2O_4 lead to the strong spin fluctuations and the heavy-fermion behavior, which are in accordance with previous experiments.[17,24] Our calculations not only shed light on understanding the exotic magnetic properties of LiV_2O_4, but also show the possibility of using the electronic structure calculations to distinguish the magnetically disordered materials from the ordered ones.

Acknowledgments

We wish to thank Rong-Qiang He, Jie Yuan, and Lei Shan for helpful discussions. Computational resources were provided by the Physical Laboratory of High Performance Computing at Renmin University of China.

References

[1] Hill R J, Craig J R and Gibbs G V 1979 *Phys. Chem. Minerals* **4** 317
[2] Johnston D C, Prakash H, Zachariasen W H and Viswanathan R 1973 *Mater. Res. Bull.* **8** 777
[3] Moshopoulou E G 1999 *J. Am. Ceram. Soc.* **82** 3317
[4] Jin K, He G, Zhang X, Maruyama S, Yasui S, Suchoski R, Shin J, Jiang Y, Yu H S, Yuan J, Shan L, Kusmartsev V F, Greene R L and Takeuchi I 2015 *Nat. Commun.* **6** 7183
[5] He G, Jia Y, Hou X, Wei Z, Xie H, Yang Z, Shi J, Yuan J, Shan L, Zhu B, Li H, Gu L, Liu K, Xiang T and Jin K 2017 *Phys. Rev. B* **95** 054510
[6] Strobel P, Cras F L, Seguin L, Anne M and Tarascon J M 1998 *J. Soild State Chem.* **135** 132
[7] Oohara Y, Sugiyama J and Kontani M 1999 *J. Phys. Soc. Jpn.* **68** 242
[8] Maitra T and Valentí R 2007 *Phys. Rev. Lett.* **99** 126401
[9] Fritsch V, Hemberger J, Büttgen N, Scheidt E W, Krug von Nidda H A, Loidl A and Tsurkan V 2004 *Phys. Rev. Lett.* **92** 116401
[10] Zhao K H, Wang Y H, Shi X L, Liu N and Zhang L W 2015 *Chin. Phys. Lett.* **32** 087503
[11] Kondo S, Johnston D C, Swenson C A, Borsa F, Mahajan A V, Miller L L, Gu T, Goldman A I, Maple M B, Gajewski D A, Freeman E J, Dilley N R, Dickey R P, Merrin J, Kojima K, Luke G M, Uemura Y J, Chmaissem O and Jorgensen J D 1997 *Phys. Rev. Lett.* **78** 3729
[12] Auerbach A and Levin K 1986 *Phys. Rev. Lett.* **57** 877
[13] Nekrasov I A, Pchelkina Z V, Keller G, Pruschke T, Held K, Krimmel A, Vollhardt D and Anisimov V I 2003 *Phys. Rev. B* **67** 085111
[14] Anisimov V I, Korotin M A, Zölfl M, Pruschke T, Hur K L and Rice T M 1999 *Phys. Rev. Lett.* **83** 364
[15] Singh D J, Blaha P, Schwarz K and Mazin I I 1999 *Phys. Rev. B* **60** 16359
[16] Arita R, Held K, Lukoyanov A V and Anisimov V I 2007 *Phys. Rev. Lett.* **98** 166402

[17] Tomiyasu K, Iwasa K, Ueda H, Niitaka S, Takagi H, Ohira-Kawamura S, Kikuchi T, Inamura Y, Nakajima K and Yamada K 2014 *Phys. Rev. Lett.* **113** 236402

[18] Hattori K and Tsunetsugu H 2009 *Phys. Rev. B* **79** 035115

[19] Yamashita Y and Ueda K 2003 *Phys. Rev. B* **67** 195107

[20] Koda A, Kadono R, Higemoto W, Ohishi K, Ueda H, Urano C, Kondo S, Nohara M and Takagi H 2004 *Phys. Rev. B* **69** 012402

[21] Ueda Y, Fujiwara N and Yasuoka H 1997 *J. Phys. Soc. Jpn.* **66** 778

[22] Kondo S, Johnston D C and Miller L L 1998 *Phys. Rev. B* **59** 2609

[23] Lee S H, Qiu Y, Broholm C, Ueda Y and Rush J J 2001 *Phys. Rev. Lett.* **86** 5554

[24] Shimizu Y, Takeda H, Tanaka M, Itoh M, Niitaka S and Takagi H 2012 *Nat. Commun.* **3** 981

[25] Burdin S, Grempel D R and Georges A 2002 *Phys. Rev. B* **66** 045111

[26] Lacroix C 2001 *Can. J. Phys.* **79** 1469

[27] Uehara A, Shinaoka H and Motome Y 2015 *Phys. Rev. B* **92** 195150

[28] Fujimoto S 2002 *Phys. Rev. B* **65** 155108

[29] Matsuno J, Fujimori A and Mattheiss L F 1999 *Phys. Rev. B* **60** 1607

[30] Eyert V, Höck K H, Horn S, Loidl A and Riseborough P S 1999 *Europhys. Lett.* **46** 762

[31] Zhang Y H, Meng J and Taft C A 2009 *Mol. Phys.* **107** 1445

[32] Rogers D B, Gillson J L and Gier T E 1967 *Solid State Commun.* **5** 263

[33] Faran O and Volterra V 1997 *Solid State Commun.* **101** 861

[34] Chmaissem O, Jorgensen J D, Kondo S and Johnston D C 1997 *Phys. Rev. Lett.* **79** 4866

[35] Mahajan A V, Sala R, Lee E, Borsa F, Kondo S and Johnston D C 1998 *Phys. Rev. B* **57** 8890

[36] Takeda H, Kato Y, Yoshimura M, Shimizu Y, Itoh M, Niitaka S and Takagi H 2015 *Phys. Rev. B* **92** 045103

[37] Krimmel A, Loidl A, Klemm M, Horn S and Schober H 1999 *Phys. Rev. Lett.* **82** 2919

[38] Fujiwara N, Yasuoka H and Ueda Y 1998 *Phys. Rev. B* **57** 3539

[39] Urano C, Nohara M, Kondo S, Sakai F, Takagi H, Shiraki T and Okubo T 2000 *Phys. Rev. Lett.* **85** 1052

[40] Jönsson P E, Takenaka K, Niitaka S, Sasagawa T, Sugai S and Takagi H 2007 *Phys. Rev. Lett.* **99** 167402

[41] Shimoyamada A, Tsuda S, Ishizaka K, Kiss T, Shimojima T, Togashi T, Watanabe S, Zhang C Q, Chen C T, Matsushita Y, Ueda H, Ueda Y and Shin S 2006 *Phys. Rev. Lett.* **96** 026403

[42] Irizawa A, Shimai K, Nanba T, Niitaka S and Takagi H 2010 *J. Phys.: Conf. Ser.* **200** 012068

[43] Chamberland B L and Hewston T A 1986 *Solid State Commun.* **58** 693

[44] Das S, Zong X, Niazi A, Ellern A, Yan J Q and Johnston D C 2007 *Phys. Rev. B* **76** 054418

[45] Johnston D C 2000 *Physica B* **281**&**282** 21

[46] Takagi H, Urano C, Kondo S, Nohara M, Ueda Y, Shiraki T and Okubo T 1999 *Mater. Sci. Eng. B* **63** 147

[47] Okabe H, Hiraishi M, Koda A, Kojima K M, Takeshita S, Yamauchi I, Matsushita Y, Kuramoto Y and Kadono R 2019 *Phys. Rev. B* **99** 041113(R)

[48] Blöchl P E 1994 *Phys. Rev. B* **50** 17953

[49] Kresse G and Joubert D 1999 *Phys. Rev. B* **59** 1758

[50] Kresse G and Hafner J 1993 *Phys. Rev. B* **47** 558

[51] Kresse G and Hafner J 1994 *J. Phys.: Condens. Matter* **6** 8245

[52] Kresse G and Furthmüller J 1996 *Comput. Mater. Sci.* **6** 15

[53] Kresse G and Furthmüller J 1996 *Phys. Rev. B* **54** 11169

[54] Perdew J P, Burke K and Ernzerhof M 1996 *Phys. Rev. Lett.* **77** 3865

[55] Blöchl P E, Jepsen O and Andersen O K 1994 *Phys. Rev. B* **49** 16223

[56] Becke A D and Johnson E R 2006 *J. Chem. Phys.* **124** 221101

[57] Tran F and Blaha P 2009 *Phys. Rev. Lett.* **102** 226401

[58] Perdew J P, Ruzsinszky A, Tao J M, Staroverov V N, Scuseria G E and Csonka G I 2005 *J. Chem. Phys.* **123** 062201

[59] Liu K, Lu Z Y and Xiang T 2016 *Phys. Rev. B* **93** 205154

[60] Yang H C, Gong B C, Liu K and Lu Z Y 2018 *J. Phys.: Condens. Matter* **31** 025803